Interdependent Risk in Interacting Infrastructure Systems

B. A. Carreras	D. E. Newman	Paul Gradney	V. E. Lynch	I. Dobson
Oak Ridge National Laboratory, Oak Ridge, TN 37831 USA carrerasba@ornl.gov	*Physics Department University of Alaska, Fairbanks, AK 99775 USA* ffden@uaf.edu	*Physics Department University of Alaska, Fairbanks, AK 99775 USA*	*Oak Ridge National Laboratory, Oak Ridge, TN 37831 USA* lynchve@ornl.gov	*ECE Department, University of Wisconsin, Madison, WI 53706 USA* dobson@engr.wisc.edu

Abstract

Critical infrastructures display many of the characteristic properties of complex systems. They exhibit infrequent large failures events that often obey a power law distribution in their probability versus size. This power law behavior suggests that conventional risk analysis does not apply to these systems. It is thought that some of this behavior comes from different parts of the systems interacting with each other both in space and time. While these complex infrastructure systems can exhibit these characteristics on their own, in reality these individual infrastructure systems interact with each other in even more complicated ways. This interaction can lead to increased or decreased risk of failure in the individual systems. To investigate this, we couple two complex system models and investigate the effect of the coupling on the characteristic properties of the systems such as the probability distribution of events.

1. Introduction

It is fairly clear that many important infrastructure systems exhibit the type of behavior that has come to be associated with "Complex System" dynamics. These systems range from electric power transmission and distribution systems, through communication networks, commodity transportation infrastructure and arguably all the way to the economic markets themselves. There has been extensive work in the modeling of some of these different systems. However, because of the intrinsic complexities involved, modeling of the interaction between these systems has been limited [1,2]. While understandable from the standard point of view that espouses understanding the components of a large complex system before one tries to understand the entire system, this approach can unfortunately overlook important consequences of the coupling of these systems that impact their safe operation and overlooks critical vulnerabilities of these systems. At the same time, one cannot simply take the logical view that the larger coupled system is just a new larger complex system because

of the heterogeneity introduced by the coupling of the systems. While the individual systems may have a relatively homogeneous structure, the coupling between the systems is often fundamentally different both in terms of spatial uniformity and in terms of coupling strength (Figure 1). This in the most extreme case leads to uncoupled systems but in the more normal region of parameter space in which the inter-system coupling is weaker or topologically different then the intra-system coupling can lead to important new behavior. Understanding the effect of this coupling on the system dynamics is necessary if we are to accurately develop risk models for the different infrastructure systems individually or collectively.
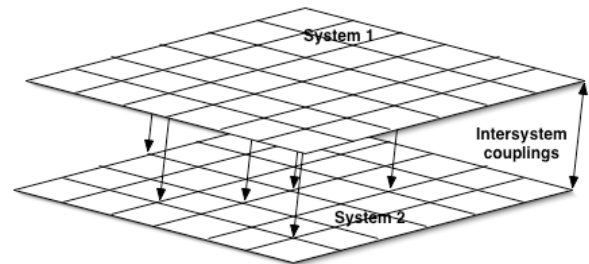

Figure 1: Cartoon of two homogeneous systems with a heterogeneous coupling

Examples of the types of potential coupled infrastructure systems to which this would be relevant include power-communication systems, power-market systems, communication-transportation systems, and even market-market systems. Interesting examples of these interactions are discussed in ref. [3]. The effect of this coupling can be critical and obvious for systems that are strongly coupled such as the power – market coupled system. Perturbations in one can have a rapid and very visible impact on the other. In fact, in many ways such systems are often thought of as one larger system even though the coupling is not homogeneous and each of the component systems (namely the market and the power transmission system) can have their own separate perturbations and dynamics. For other less tightly coupled systems, such as power-communications systems, the effect can be much more subtle but still very important. In such

systems small perturbations in one might have very little obvious effect on the other system, yet the effect of the coupling of the two systems can have a profound effect on the risk of large, rare disturbances.

In this paper, we will present results from a dynamical model of coupled complex systems. This model has dynamic evolution and many of the characteristics found in complex systems.

Many complex systems are seen to exhibit similar characteristics in their failures. While it is useful and important to do a detailed analysis of the specific causes of these failures such as the failure sequence for individual blackouts, it is also important to understand the global dynamics of the systems like the power transmission network. This allows some insight into the frequency distribution of these events (e.g. blackouts) that the system dynamics creates. There is evidence that global dynamics of complex systems is largely independent of the details of the individual triggers such as shorts, lightning strikes etc in power systems. In this paper, we focus on the intrinsic dynamics of failures and how this complex system dynamics impacts failure risk assessment in interconnected complex systems. It is found, perhaps counter intuitively, that even weak coupling of complex systems can have adverse effects on both systems and therefore risk analysis of an isolated system must be approached with care.

Several particular issues induced by the interdependence of systems will be addressed in this paper. The first one is how coupling between the systems modifies conditions for safe operation. These systems are characterized by a critical loading [4, 5]. They must operate well below this critical loading to avoid "normal accidents" [6] and large-scale failures. We will explore how the coupling between systems changes the value of this critical loading.

We will also consider the effect of the heterogeneity introduced through in two different ways, first through the different properties of each individual system, such as having different critical points, and second, through the coupling of the systems.

The rest of the paper will be organized as follows: Section 2 reviews some of the characteristics of complex systems. Section 3 describes the dynamic model with results from that model, followed by section. Section 4 describes the mean field results for the dynamic model, followed by sections 5 and 6 that describe results from identical coupled systems and asymmetric systems respectively. Finally, section 7 discusses the character of the transcritical bifurcation and section 8 has a discussion of the implications of these results and conclusions.

2. Background

The following work is a continuation of previous work on the Demon model of coupled infrastructure systems [7]. Here, we will extend the model to consider arbitrary network structures. The previous work was centered on a square grid network. Therefore the basic coupling was from each node to four neighbors. The model was a simple extension of Drossel model [8] for forest fires. In this model, the propagation velocity of a disturbance is $P_n f$ where P_n is the probability of

a disturbance to propagate from a node to another node and f the number of available nodes to propagate from a given node. In this model f is an important parameter to understand the propagation of the disturbances and it is not well determined. If K is the averaged number of nodes coupled to a single node in a given network, a first guess for f is $f = K–1$, because the disturbance is already coming from one of the nodes that the failing node is coupled. In the case of the square network it has been found that f = 2.66 is a better value than 3. Therefore, we will vary K in order to understand what are possible values for f.

To do so, we consider several network structures. In Fig. 2a, we show an example of two coupled hexagon-like networks during the development of a cascading failure. The green nodes represent operating components of the system. A similar plot in Fig. 2b shows two coupled open tree networks

Another aspect to explore is how the power law of the pdf of failures depends on K, if it does at all.

Finally the more interesting new aspect to explore is the coupling of heterogeneous networks with different K and number of nodes. In practical problems of interdependence between infrastructure systems, each infrastructure has its own structure and the ways two of them are coupled are non-uniform. We will use the Demon model in studying this situations and understanding the propagation of disturbance in these heterogeneous systems.
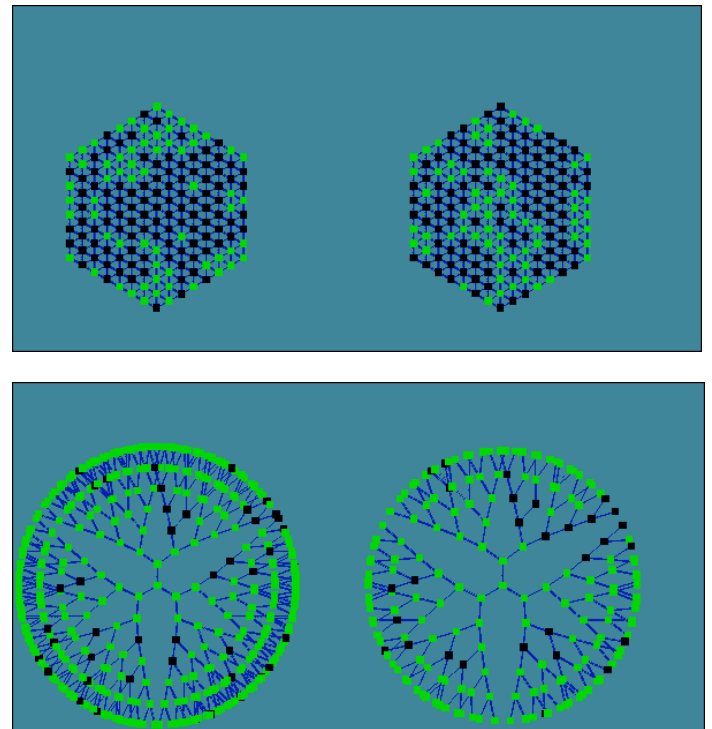

Figure 2a: Two coupled hexagon systems during cascading failure. Figure 2b : Two coupled tree systems during cascading failure coupling

In all these studies, we will be using the mean field theory for the coupled systems developed in ref. [7] as guidance and we will investigate its effectiveness and limitations.

3. The Demon model

The infrastructure model discussed here, the Demon model, is based on the forest fire model of Bak, Chen and Tang [9] with modifications by Drossel and Schwabl [8].

For a single system, the model is defined on a 2-d network. Examples of such networks are shown in Figs. 1 and 2. In Table I we have summarized the properties of the different networks considered. Nodes represent components of the infrastructure system and lines represent the coupling between components. These components can be operating, failed or failing. The rules of the model are for each time step are:

1) A failed component is repaired with probability P_r.

2) A failing component becomes a failed one

3) An operating component fails with probability P_n if at least one of the nearest components is failing.

4) There is a probability P_f that any operating component fails.

We consider a coupled system by taking two of these 2-d networks and adding another rule:

5) A component fails in System 1 fails if the associated component in System 2 is failed or failing. The same applies for a component in system 2.

Using these rules, numerical calculations can be carried out. We will consider first the mean field theory for this model and in later sections we will discuss the numerical results.

Table I Network properties

Type	K	Number of nodes
Open 3-branch Tree	2	3070
Closed 3-branch Tree	3	3070
Open 5-branch Tree	4	190
Square	3.96	10000
Hexagon	5.9	4681

4. Mean field theory: steady state

Let us consider first the mean field theory for two coupled systems. This is a generalization of the calculation done in Ref. [8]. Let $O^{(i)}(t)$ be the number of operating components in system i at time t normalized to the total number of components $N^{(i)}$. In the same way, we can define the normalized number of failed components, $F^{(i)}(t)$, and the failing ones, $B^{(i)}(t)$. The mean field equations for this coupled system are:

$$B^{(1)}(t+1) = P_f^{(1)}O^{(1)}(t) + P_n^{(1)}f^{(1)}O^{(1)}(t)B^{(1)}(t)$$
$$+ \frac{c^{(1)}}{\kappa}g_2 O^{(1)}(t)\left(B^{(2)}(t) + F^{(2)}(t)\right)$$
(1)

$$F^{(1)}(t+1) = \left(1 - P_r^{(1)}\right)F^{(1)}(t) + B^{(1)}(t)$$
(2)

$$O^{(1)}(t+1) = \left(1 - P_f^{(1)}\right)O^{(1)}(t) + P_r^{(1)}F^{(1)}(t)$$
$$- P_n^{(1)}f^{(1)}O^{(1)}(t)B^{(1)}(t)$$
$$- \frac{c^{(1)}}{\kappa}g_2 O^{(1)}(t)\left(B^{(2)}(t) + F^{(2)}(t)\right)$$
(3)

$$B^{(2)}(t+1) = P_f^{(2)}O^{(2)}(t) + P_n^{(2)}f^{(2)}O^{(2)}(t)B^{(2)}(t)$$
$$+ \kappa c^{(2)}g_1 O^{(2)}(t)\left(B^{(1)}(t) + F^{(1)}(t)\right)$$
(4)

$$F^{(2)}(t+1) = \left(1 - P_r^{(2)}\right)F^{(2)}(t) + B^{(2)}(t)$$
(5)

$$O^{(2)}(t+1) = \left(1 - P_f^{(2)}\right)O^{(2)}(t) + P_r^{(2)}F^{(2)}(t)$$
$$- P_n^{(2)}f^{(2)}O^{(2)}(t)B^{(2)}(t)$$
$$- \kappa c^{(2)}g_1 O^{(2)}(t)\left(B^{(1)}(t) + F^{(1)}(t)\right)$$
(6)

Here $\kappa \equiv N^{(1)}/N^{(2)}$, g_1 is the fraction of nodes in system 1 coupled to system two, and g_2 is the fraction of nodes in system 2 coupled to system 1. Of course, these equations are consistent with the conditions:

$$O^{(i)}(t) + B^{(i)}(t) + F^{(i)}(t) = 1$$
(7)

In the limit with no failure triggers, $P_f^{(i)} = 0$, and for a steady state solution, the system of equations can be reduced to two coupled equations,

$$\left[1 - P_n^{(1)}f^{(1)}O^{(1)}\right]\left(1 - O^{(1)}\right) = \frac{a^{(1)}}{\kappa}g_2\left(1 - O^{(2)}\right)O^{(1)}$$
(8)

$$\left[1 - P_n^{(2)}f^{(2)}O^{(2)}\right]\left(1 - O^{(2)}\right) = \kappa a^{(2)}g_1\left(1 - O^{(1)}\right)O^{(2)}$$
(9)

where

$$a^{(i)} = \frac{c^{(i)}\left(1 + P_r^{(i)}\right)}{P_r^{(i)}}$$
(10)

It is important to note that the relevant parameter involves the ratio of the coupling between the systems and the repair rate. The reason for that is the particular form of rule 5) that assumes that a failure can be triggered by both failed and failing components in the other system. If only failing

components had been considered, the relevant parameter would be the coupling. For real systems, a realistic rule should probably lie in between these two extremes.

If $a^{(i)} \neq 0$ and $\kappa = 1$, then $O^{(1)} = 1$ implies $O^{(2)} = 1$, that is, the systems are decoupled. Therefore, to have truly coupled systems, system 1 must be in a supercritical state. Such a case with $a^{(i)} \neq 0$ is more complicated to solve.

First, we have assumed identical systems symmetrically coupled. That is, all parameters are the same for the two systems, $f^{(1)} = f^{(2)}$, $a^{(1)} = a^{(2)}$, $\kappa = 1$ and $P_n^{(1)} = P_n^{(2)}$. This leads to identical solutions for the two systems in steady state. Therefore, we have the following stable solutions:

$$O^{(i)} = \begin{cases} 1 & for \quad \hat{g} \leq 1 \\ \dfrac{1}{\hat{g}} & for \quad \hat{g} > 1 \end{cases} \tag{11}$$

$$F^{(i)} = \begin{cases} 0 & for \quad \hat{g} \leq 1 \\ \dfrac{\hat{g}-1}{\hat{g}(1+P_r)} & for \quad \hat{g} > 1 \end{cases} \tag{12}$$

$$B^{(i)} = \begin{cases} 0 & for \quad \hat{g} \leq 1 \\ \dfrac{\hat{g}-1}{\hat{g}(1+P_r)} P_r & for \quad \hat{g} > 1 \end{cases} \tag{13}$$

Here, $\hat{g}$ is the control parameter and is given by

$$\hat{g} = P_n f + \frac{c(1+P_r)}{P_r} \tag{14}$$

5. Coupling of two identical systems

We have tested the results from the mean field theory by comparing them with numerical results from some of the two-coupled identical systems networks listed in Table I. The results for the averaged number of operating components are shown in Fig. 3. Results have been obtained for fixed $P_r = 0.001$, $c = 0.0005$, and $P_f = 0.00001$ and we have varied the propagation parameter P_n. The results show very good agreement with the mean field theory results as K increases. For $K = 2$, the system are practically 1–d and the mean field theory is not really applicable.

The density of operating components is practically the same in both systems. This is logical because they are identical systems and the only symmetry-breaking feature is the probability of spontaneous failures that is zero in the second system.
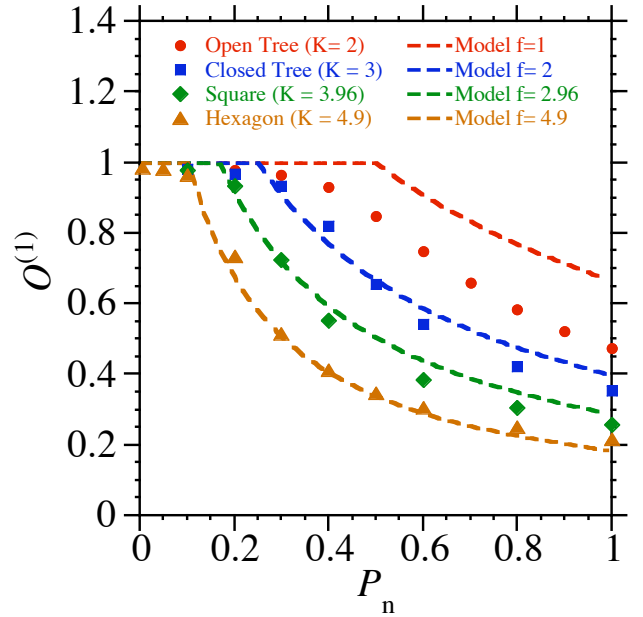

Figure 3: Fraction of operating components for various configurations.

Near the critical point the pdf of the sizes are similar with a power law region with exponent close to -1. For the forest fire model, which corresponds to the present model for the uncoupled square grid, Drossel et al [8] showed that the exponent is -1. Here we need to do more detailed calculations in the limit of large grid and small probability of random failure in order to understand those exponents. In Fig. 4, we show an example of the pdf of failure sizes for three different coupled network structures.
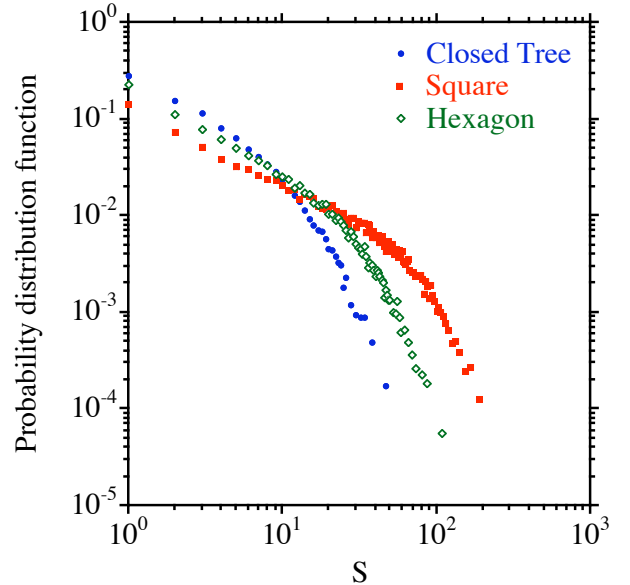

Figure 4: PDFs for 3 coupled systems

Perhaps most important is the effect of the coupling of the systems on the point at which the power law tails develop, the so called critical point. The point is characterized by the P_n value at which the percolation transition occurs as discussed earlier. This point can be measured in a variety of ways, including changes in the equilibrium state as discussed

in the mean field calculations and changes in the propagation characteristics as discussed in section 6. These different measures give different critical points and even slightly different functional dependencies on the coupling strength. These differences will be discussed elsewhere. Figure 5 shows the change in the critical propagation parameter P_n as a function of the coupling strength as measured from the density of unfailed components. The relationship is not a linear dependency and is consistent with a weak power law function with an exponent of approximately -0.4. This shows that the impact of even a very small coupling between systems can be significant. The same result, characterized using the propagation measure λ (as discussed later in section 6) gives a similar figure with an offset in the actual value of the critical point varying between 0.05 and 0.1 and a weaker low coupling dependence.
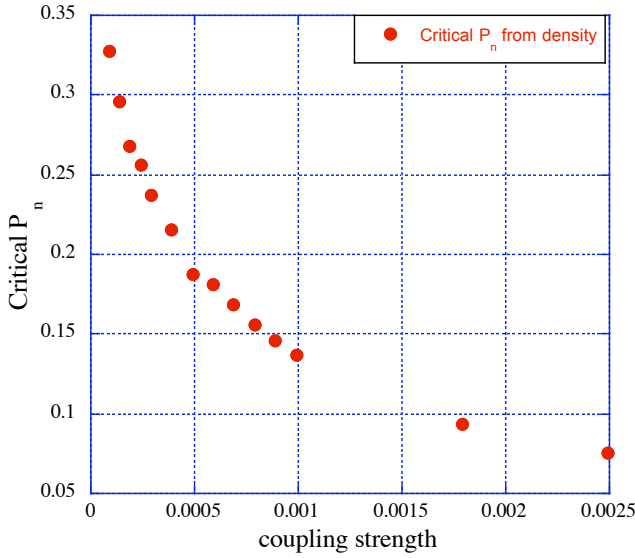

Figure 6: Coupled asymmetric systems with symmetry broken by course graining one system.

First, we use the same parameters for both squares, in particular $P_r = 0.001$, c = 0.0005, and $P_f = 0.00001$. Results for the densities of operating components are shown in Fig. 7.

Figure 5: Critical P_n as coupling strength c varies

Figure 7: Analytic and computational results for operating components with asymmetric system configurations

6. Coupling of different systems

Let us start from two squares with different numbers of nodes. This is the simplest way of breaking the symmetry between systems. We choose the geometrical dimensions of the systems to be the same and the number of nodes on a side of the square to be a multiple of the other. Therefore, we couple only the nodes that geographically are on top of each other. We have used a 100x100 square coupled to a 20x20 square and to a 50x50 square. An example of the first pair of grids is shown in Fig. 6 at a given time during the evolution. The green nodes represent working components and the black ones the failed components.
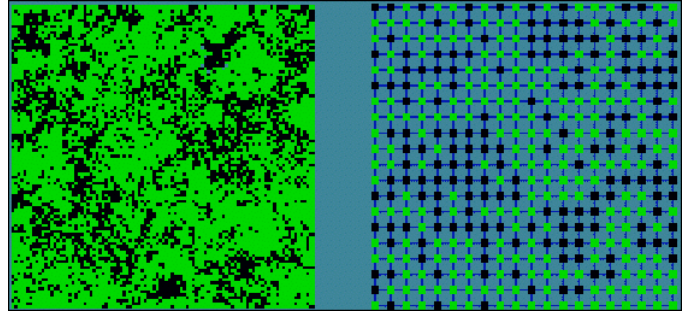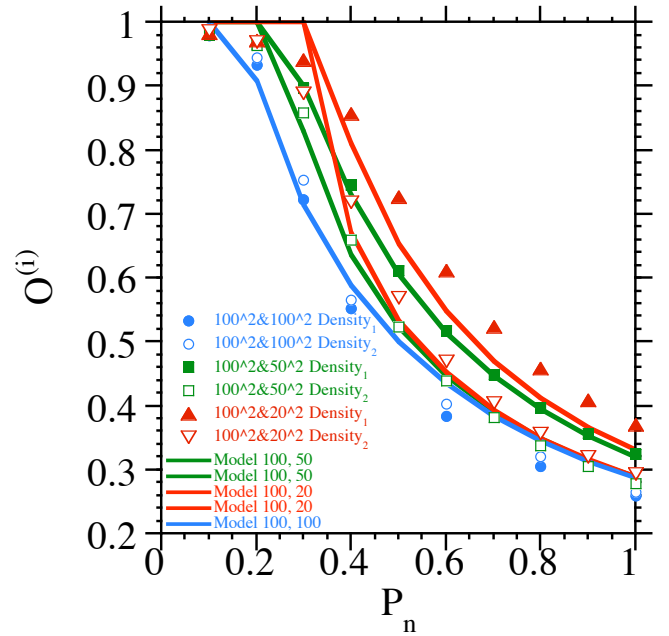
Now the densities of the operating components are not the same in the two systems. In this calculation System 1 was the 100x100 square and System 2 the square with less nodes. System 2 has normally a lower density of operating components. Numerical results compare well with the mean field theory. For this problem, the corresponding version of Eqs. (8) and (9) are

$$\left[1 - P_n f\, O^{(1)}\right]\left(1 - O^{(1)}\right) = \frac{1}{\kappa} a\left(1 - O^{(2)}\right)O^{(1)} \qquad (15)$$

$$\left[1 - P_n f O^{(2)}\right]\left(1 - O^{(2)}\right) = a\,\kappa\left(1 - O^{(1)}\right)O^{(2)} \qquad (16)$$

where κ is the ratio of the number of nodes in the large system to the number of nodes in the small system. Now these equations cannot be solved analytically but they are easily solved numerically. The results for the two-coupled

cases considered here are plotted in Fig. 7 and compared with the numerical results.

We have also made a scan in the coupling coefficient c and compared the mean field theory and numerical results in Fig. 8.
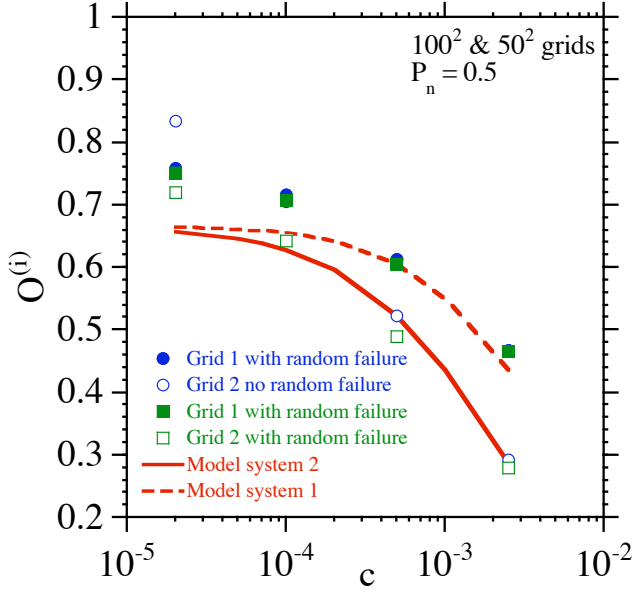

Figure 8: Fraction of operating components vs. coupling coefficient.

The comparison is good for large coupling coefficients. At small values the coupling starts competing with the random triggers. For one of the numerical calculations only system 1 has random failures, therefore the density of operating components in system 2 goes to one when the coupling goes to zero. In the second calculation there are random failures in both grids. In this case the two grids converge to the same value as the coupling goes to zero.

7. The critical point as a transcritical bifurcation

The critical point of the mean field model (1)-(6) at $\hat{g}$ = 1 can be understood as a transcritical bifurcation. The model (1) - (6) has two equilibria

$$\left(O_1^{(1)}, F_1^{(1)}, B_1^{(1)}\right) = \left(1, 0, 0\right) \qquad (17)$$

$$\left(O_2^{(1)}, F_2^{(1)}, B_2^{(1)}\right) = \left(\frac{1}{\hat{g}}, \frac{\hat{g}-1}{\hat{g}(1+P_r)}, \frac{\hat{g}-1}{\hat{g}(1+P_r)}P_r\right) \qquad (18)$$

The equilibria coincide at $\hat{g}$ = 1 and as $\hat{g}$ increases through 1 the second equilibrium passes through the fixed first equilibrium. For the subcritical case $\hat{g}$ < 1, the first equilibrium is stable and the second equilibrium is nonphysical since $O^{(i)}$ > 1. For the supercritical case $\hat{g}$ > 1, the second equilibrium is stable and the first equilibrium is unstable. At the critical case of $\hat{g}$ = 1, the linearization at the bifurcating equilibrium has an eigenvalue of one.

To confirm these claims, we choose the state vector to be $(B^{(1)}, F^{(1)}, B^{(2)}, F^{(2)})$ and use (7) to eliminate $O^{(i)}$ in (1), (2), (4), (5). The parameters chosen are κ = 1, $N_1 = N_2$, $c^{(1)} = c^{(2)} = c$, $\hat{g}_1 = \hat{g}_2 = \hat{g}$, $f^{(1)} = f^{(2)} = f$, $P_f^{(1)} = P_f^{(2)} = 0$, $P_r^{(1)} = P_r^{(2)} = P_r$. We then linearize (1), (2), (4), (5) about the first equilibrium and compute the maximum eigenvalue to be

$$\lambda_{max1} = \frac{1}{2}\left(1 - P_r + P_n f + c + \sqrt{\left(1 - P_r - P_n f - c\right)^2 + 4c}\right)$$

This eigenvalue goes through 1 when $\hat{g}$ =1.

An issue remains whether this bifurcation point is directly related to the cascading threshold. To measure the cascade propagation we measure

$$\lambda_B\left(t\right) = \frac{B(t)}{B(t-1)}$$

It is interesting to measure this λ_B in the two different systems. An example is shown in Fig. 9. Systematically, the λ_B measure in the small system is below 1 while in the large system becomes greater than 1 at a critical point.
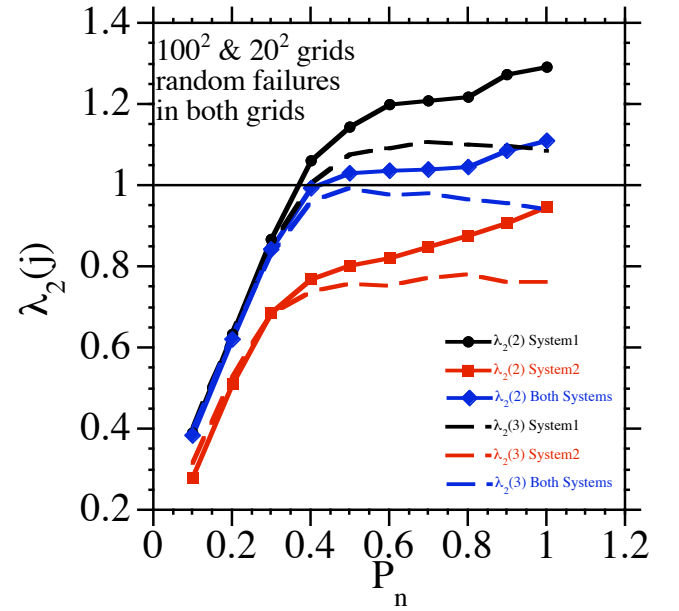

Figure 9: λ plotted across critical point for both systems.

Therefore, an operator in the small system just by measuring failures in their system feels that it is in a safe operation regime when he is not. This result emphasizes the need for a global parameter that describes the status of the overall system.

One can see that both systems are supercritical in spite of the values of l, by looking at the pdf of the size of the events. In Fig.10 we have plotted an example of such pdf. It includes the one measured in the system 1, the one in system 2, and the one combined. The there exhibit a clear power law region with exponential tail as is typical in the coupling of identical systems.
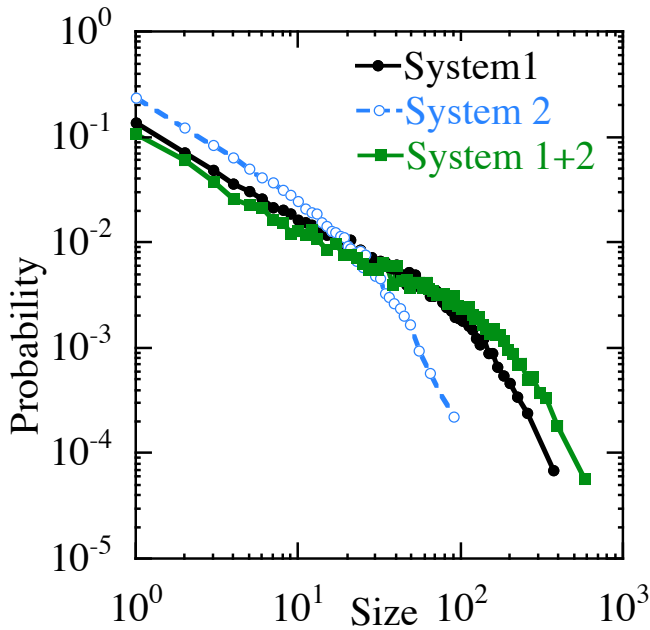
Figure 10: Power law PDF for both systems suggests both critical despite $\lambda < 1$.

8. Discussion and Conclusions

Modern societies rely on the smooth operation of many of the infrastructure systems. We normally take them for granted. However, we are typically shocked when one of these systems fails. Therefore, understanding these systems is a high priority for ensuring security and social wellbeing. Because none of these infrastructure systems operate in a vacuum, understanding how these complex systems interact with each other gains importance when we recognize how tightly coupled some of these systems are. Because of the great complexity of even the individual systems it is unrealistic to think that we can dynamically model interacting infrastructure systems in full detail at present.

In this paper, we have investigated some of the general features of interactions between infrastructure systems by using very simple models. We look for general dynamical features without trying to capture the details of the individual systems. In the future we will try to build a hierarchy of models with increasing levels of detail for these systems.

Here, we have explored the Demon model, which can work in a self-organized critical state. The Demon model has a percolation threshold above which cascading failures of all sizes are possible. It has been found that symmetric coupling of these systems actually decreases the threshold nonlinearly. That is, it makes access to the critical point easier, which means that the systems when coupled are more susceptible to large-scale failures and a failure in one system can cause a similar failure in the coupled system. The parameter λ, can be also used to characterize the cascading threshold in the coupled systems. This suggests the existence of a metric that can be generalized for practical application to more realistic systems.

For the Demon model it is found that large failures are more likely to be "synchronized" across the two dynamical systems, which is likely to be the reason that the power law found in the probability of failure with size becomes less steep as the coupling increases. This means that in the coupled systems there is greater probability of large failures and less probability of smaller failures.

With the Demon model other important aspects of the infrastructure can be explored, such as non-uniform and non-symmetric couplings. This will be the object of future studies.

With this model there is a large parameter space that must be explored with different regions of parameter space having relevance to different infrastructure systems. There is also a rich variety of dynamics to be characterized. Characterizing the dynamics in the different regimes is more then an academic exercise since as we engineer higher tolerances in and otherwise optimize individual systems as well as making the interdependencies between systems stronger we will then be exploring these new parameter regimes of the coupled systems the hard way, by trial and error. Unfortunately error in this case has the potential to lead to global system failure. By investigating these systems from this high level, we hope that regimes to be avoided can be identified and mechanisms for avoiding them can be explored.

References

[1] R. G. Little, Toward more robust infrastructure: Observations on improving the resilience and reliability of critical systems, 36th Annual Hawaii International Conference on System Sciences, Hawaii, January 2003.

[2] S.M. Rinaldi, Modeling and simulating critical infrastructures and their interdependencies, 37th Annual Hawaii International Conference on System Sciences, Hawaii Jan. 2004.

[3] S.M. Rinaldi, J. P. Peerenboom, and T. K. Kelly, Identifying, understanding, and analyzing critical infrastructure interdependencies, IEEE Control Systems Magazine, p. 11, December 2001.

[4] B.A. Carreras, V.E. Lynch, I. Dobson, D.E. Newman, Critical points and transitions in an electric power transmission model for cascading failure blackouts, Chaos, vol. 12, no. 4, December 2002, pp. 985-994.

[5] I. Dobson, J. Chen, J.S. Thorp, B. A. Carreras, and D. E. Newman, Examining criticality of blackouts in power system models with cascading events, 35th Hawaii International Conference on System Sciences, Hawaii, Hawaii, Jan. 2002.

[6] C. Perrow, *Normal accidents*, Princeton University Press, 1984.

[7] D. E. Newman, B. Nkei, B. A. Carreras, I. Dobson, V. E. Lynch, P. Gradney, Risk assessment in complex interacting infrastructure systems, Thirty-eighth Hawaii International Conference on System Sciences, Hawaii, January 2005

[8] B. Drossel and F. Schwabl, Forest-fire model with immune trees, Physica A, vol. 199, pp. 183-197 1993.

[9] P. Bak, K. Chen and C. Tang, A forest-fire model and some thoughts on turbulence, Physics Letters A, vol. 147, pp. 297-300, 1990.